ChemComm

COMMUNICATION

Regio Selective Deposition of Conducting Polymers using Wireless Electropolymerisation

Received 00th January 20xx,
Accepted 00th January 20xx

DOI: 10.1039/x0xx00000x

Áine Brady,[a] Michal Wagner,[a] and Robert Forster [a,b] *

The ability to induce different potentials in different regions of a (bipolar) electrode could be transformative for many applications such as on-demand drug delivery, the stimulation of biological cells towards the development of advanced electroceuticals, and for multi-analyte detection devices where *different analytes* could be *wirelessly* detected in different regions of a *single* sensing surface dramatically simplifying the device design. Here, we demonstrate the use of *multiple* feeder electrodes to control the electric field distribution in solution thus changing the potential induced in different regions of the bipolar electrode depending on the voltage applied, polarity and feeder electrode position. This allows for deposition of films of the conducting polymer, PEDOT, without the need for a physical template to control the regions in which polymer deposits.

Bipolar, or wirefree, (BP) electrochemistry [1–3] uses feeder/ or driving electrodes to create an electric field in solution that can induce a potential within a conductor.[4] This approach enables many applications such as the creation of Janus particles, conducting polymers, nanoscale interconnects and the electrical, electrochemical and on demand, chemical stimulation of biological cells which is vital for the emerging field of electroceuticals.[5,6] Typically, a conducting bipolar electrode (BPE) is placed between a pair of feeder electrodes and the voltage induced varies approximately linearly across the BPE. The magnitude of the voltage depends on the voltage applied to the feeder electrodes, the electrolyte concentration, and the dimensions of the BPE.[4,7]

In this work, we demonstrate that the electric field distribution in solution, and hence the potential induced in different regions of the BPE, can be shaped using more than two feeder electrodes (Figure 1). The use of multiple feeder electrodes allows the induced voltage to be controlled in 2D, and ultimately in 3D, driving different redox reactions in different regions of the BPE. This ability is highly attractive for diverse applications, e.g., to drive different electrochemiluminescent reactions (due to the different induced voltages) at different locations enabling multianalyte detection at a single unstructured electrode, to release encapsulated drugs at different rates across a conducting surface or to rapidly identify the optimum electrostimulation conditions for biological cells.[5,8–11] Here, the electrodeposition of Poly(3,4-EthyleneDiOxyThiophene) (PEDOT) is used to map the electric field in two four-feeder configurations, resulting in unique polymerisation patterns on the BPE. This regioselective electrodeposition is intended to enable template-free patterning of the polymer film.[4]

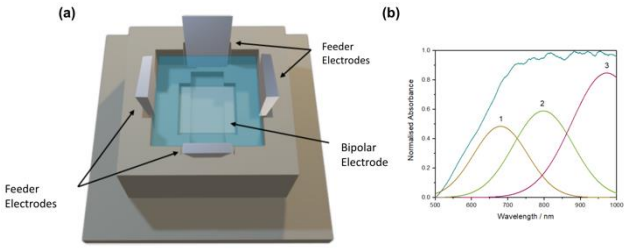

Figure. 1. (a) Diagram of the 3D printed BP cell printed in ABS with four titanium feeder electrodes (H: 2 cm x L: 1 cm x D: 2 mm) and an FTO BPE (1.5 cm x 1.5 cm). (b) UV-Vis spectrum of the wirelessly polymerised BP film at 10 V cm^{-1} for 20 minutes in 10 mM EDOT in Milli-Q water solution.

[a] School of Chemical Sciences, Dublin City University, Dublin 9, Ireland
[b] FutureNeuro, SFI Research Centre for Chronic and Rare Neurological Diseases, Dublin City University, Dublin 9, Ireland

While electrophoretic mass transport processes may be important at high field strengths, PEDOT deposition can be used

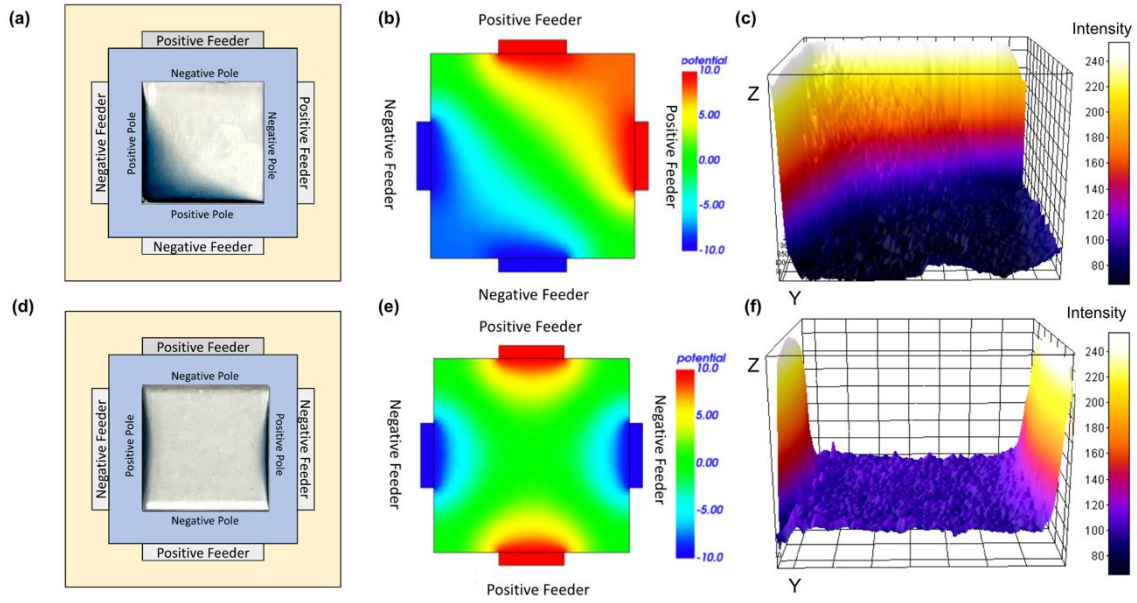

to map the electric field distribution since the voltage dependent rate of heterogeneous electron transfer impacts the polymerisation rate and hence the quantity of polymer deposited.[12] The four-feeder setup consisted of four titanium feeder electrodes (H: 2 cm x L: 1 cm x D: 2 mm) which were connected to an EA PS 5200-02A power supply (field strength of 10 V cm^{-1}) and a fluorine-doped tin oxide (FTO) BPE (1.5 cm x 1.5 cm). The solution contained 10 mM EDOT in Milli-Q water in the absence of deliberately added electrolyte. The acrylonitrile butadiene styrene (ABS) BP cell was designed using FreeCAD and printed using an Ultimaker S5 3D printer. Figure 1(a) shows the four-feeder BP setup.

Figure 2. FTO BPE polymerised in 10 mM EDOT Milli-Q water solution at V cm^{-1} for 20 minutes. (a-c) Configuration 1: (a) Positive and negative feeders oppose each other (b) FEM model of the potential distribution (blue -10 V, red +10 V) (c) 3D representation of PEDOT deposition (d-f) Configuration 2: Positive and negative feeder electrodes are adjacent to one another (e) FEM model of the potential distribution (f) 3D representation of PEDOT deposition.

The absence of deliberately added electrolyte maximises the voltage available to generate an electric field in solution and opens the possibility of creating low doped or even undoped PEDOT films. UV-Vis spectroscopy was performed on the wirelessly deposited films to provide information on the band gaps and chemical composition (Figure 1 (b)). Significantly, the experimental spectrum can be fitted with three gaussian peaks and the likely presence of polaronic absorption peaks at 680 nm, 800 nm, and 1000 nm suggests that the PEDOT is in fact 'doped'.[13,14] This is particularly interesting considering that conductivity measurements of the solution is in the μS cm^{-1} range and increase by less than 25% after the electric field is applied at 10 V cm^{-1} for 20 minutes. This suggests that relatively few ions are produced during electrodeposition. The conductivity of the solution after film deposition is equivalent to that found for a 1 nM solution of a monovalent salt and is most likely due to the release of protons as the EDOT polymerises, e.g. the formation of an EDOT dimer releases two protons.

The four-feeder BP system (two positive and two negative feeder electrodes) modifies the expected linear potential profile across the BPE when only two feeders are used. Figure 2 shows the impact of two different configurations of the four feeder electrodes on the electropolymerisation of EDOT. Figure 2 (a) has the two pairs of positive and negative feeder electrodes directly opposite one another and shows a photograph of the resulting film that is formed. Finite Element Modelling (FEM) was performed using Elmer software and the corresponding solution potential distribution is shown in Figure 2 (b). In sharp contrast to the wedge-like deposition pattern found for a single pair of feeder electrodes, PEDOT is deposited in an arc centred at the corner opposite the two negative feeder electrodes demonstrating the ability to shape the PEDOT deposition in a regio selective manner without the need for a template. The analysis of the SEM images, shows that, not only is the film structured in 2D, but the deposition occurs in a gradient with the film being thickest in the corner where the

induced voltage is highest and tapering down as the centre of the BPE is approached.

Figures 2 (d) and (f) demonstrate the high degree of control that can be exerted over the deposition region by simply changing the position of the feeder electrodes. Here, the pairs of positive and negative feeder electrodes are positioned adjacent rather than opposite one another. PEDOT deposition now occurs in two separate locations taking the form of two shallow arcs at the two positive poles of the BPE. From both the photograph and the SEM image analysis, it is clear that there is a gradient in the thickness of the deposited film, i.e., thickest at the edge and becoming thinner towards the centre of the BPE. Significantly, these results show that through a simple change in the feeder configuration, a completely different electric field is generated, enabling electrodeposition in different regions of the BPE. The

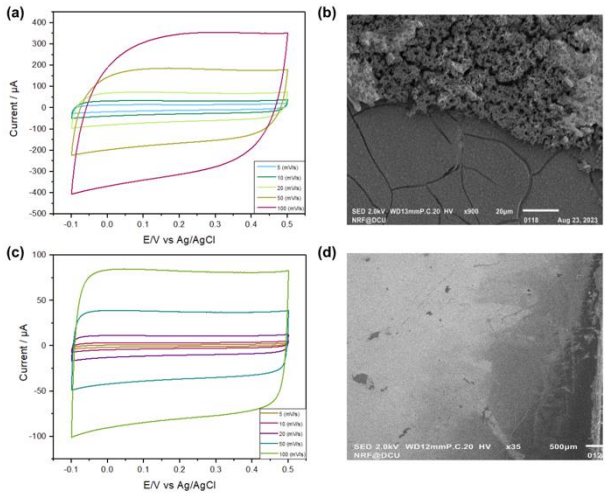

structuring of the PEDOT film correlates strongly with the FEM modelling allowing the configuration of a set of feeders to be identified *a priori* in order to give a conducting polymer film with the required topography.

Figure 3. (a) Scan rate dependent voltammetry (bottom to top, 5 to 100 mV s^{-1}) where the working electrode in a 3-electrode cell is the PEDOT coated BPE deposited using Configuration 1. (b) SEM imaging of PEDOT film formed using Configuration 1. (c) Scan rate dependent voltammetry (bottom to top, 5 to 100 mV s^{-1}) where the working electrode in a 3-electrode cell is the PEDOT coated BPE deposited using Configuration 2. (d) SEM imaging of PEDOT formed in Configuration 2. In both (a) and (c) the supporting electrolyte is 0.1 M $LiClO_4$ and the films were formed using 10 mM EDOT in Milli-Q water solution at 10 V cm^{-1} for 20 minutes.

To quantify the amount of PEDOT deposited on the BPE, a scan rate study ($5 \leq \upsilon \leq 100$ mV s^{-1}) was performed. Figure 3 (a) and (c) show the flat and featureless cyclic voltammograms are observed for both Configurations 1 and 2, which is consistent with the capacitive behaviour of PEDOT. The capacitance was calculated by plotting the current at 0.2 V versus scan rate and obtaining the slope of the best fit line. The calculated film capacitance for Configuration 1 was 2.33 mF cm^{-2} and 0.58 mF cm^{-2} for Configuration 2. The observation that the number of moles of PEDOT deposited is significantly lower (approximately 4-fold) for Configuration 2 than Configuration 1 is expected on the basis of the FEM modelling. The FEM model predicts that the fractional area of the BPE that will achieve a sufficiently positive potential to oxidise EDOT is smaller for Configuration 2 than for 1.

In Configuration 1, PEDOT is deposited at the corner of the two positive poles on the BPE and Figure 3(b) shows an SEM image. (At the edge, the film consists of globular aggregates due to higher deposition rates associated with a more positive induced potential. Significantly, there is a rather abrupt transition between the thick film at the corner and the thinner, more smooth and dense film toward the centre of the FTO. The cracks present are consistent with drying induced stress.[15] A change in film thickness is expected on the basis of the FEM potential distribution mapping, as the potential decreases from the two positive BPE poles to the diagonal centre of the BPE (Figure 2 (b)). The ImageJ generated 3D deposition (from photographs) also correlates with the SEM imaging as the film thickness is decreasing toward the centre of the BPE (Figure 2 (c)). Figure 3 (d) shows the wirelessly polymerised PEDOT film using the second four-feeder setup (Configuration 2). Consistent with the smaller number of moles deposited (approximately 4-fold) and correspondingly lower deposition rate, this film has a substantially smoother morphology, with a film thickness gradient from the edge of the FTO slide (positive pole). The gradient arc deposition can be seen as the film thickness decreases toward the centre of the BPE.

In summary, this work successfully demonstrates that i) multiple feeder electrodes can be used to wirelessly induce different potentials at different locations at a bipolar electrode in a regio selective manner, ii) the potentials can be modelled using FEM, iii) the controlled induced potentials can be used for regio selective, wirefree, electrodeposition of patterned PEDOT films without the use of a physical template. These patterned films, created using the shaped electric fields generated using multiple, purposefully positioned feeder electrodes, could enable multi-analyte detection devices, spatially controlled on-demand drug delivery, and the stimulation of biological cells toward 3D electroceuticals.

Conflicts of interest

There are no conflicts to declare.

Data availability

The data supporting the findings of this study are available within the article.

Acknowledgements.

The financial; support of Science Foundation Ireland (SFI) under Grant Number 21/FFP-P/10255 and the European Union under MSCA Doctoral network Horizon Europe programme Grant Agreement Number 101119951 (ECLectic) is gratefully acknowledged. This publication has emanated from research supported in part by a research grant from Science Foundation Ireland (SFI) under Grant Number 21/RC/10294_P2 and co-funded under the European Regional Development Fund and by FutureNeuro industry partners.

Notes and references

1 L. Koefoed, S. U. Pedersen and K. Daasbjerg, *Curr. Opin. Electrochem.*, 2017, **2**, 13–17.
2 R. M. Crooks, *ChemElectroChem*, 2016, **3**, 357–359.
3 S. E. Fosdick, K. N. Knust, K. Scida and R. M. Crooks, *Angew. Chem. Int. Ed.*, 2013, **52**, 10438–10456.
4 R. J. Forster, *Curr. Opin. Electrochem.*, 2023, **39**, 101297.
5 A. Jain, J. Gosling, S. Liu, H. Wang, E. Stone, S. Chakraborty, P.-S. Jayaraman, S. Smith, D. Amabilino, M. Fromhold, Y.-T. Long, L. Pérez-García, L. Turyanska, R. Rahman and F. Rawson, *Nat. Nanotechnol.*, , DOI:10.1038/s41565-023-01496-y.
6 A. Robinson, A. Jain, H. Sherman, R. Hague, R. Rahman, P. Sanjuan Alberte and F. Rawson, *Adv. Ther.*, 2021, **4**, 2000248.
7 C. A. C. Sequeira, D. S. P. Cardoso and M. L. F. Gameiro, *Chem. Eng. Commun.*, 2016, **203**, 1001–1008.
8 C. Qin, Z. Yue, Y. Chao, R. J. Forster, F. Ó. Maolmhuaidh, X.-F. Huang, S. Beirne, G. G. Wallace and J. Chen, *Appl. Mater. Today*, 2020, **21**, 100804.
9 E. Villani, N. Shida and S. Inagi, *Electrochimica Acta*, 2021, **389**, 138718.
10 K. Krukiewicz, A. Kruk and R. Turczyn, *Electrochimica Acta*, 2018, **289**, 218–227.
11 B. Alshammary, F. C. Walsh, P. Herrasti and C. Ponce de Leon, *J. Solid State Electrochem.*, 2016, **20**, 839–859.
12 N. Shida and S. Inagi, *Chem. Commun.*, 2020, **56**, 14327–14336.
13 I. Zozoulenko, A. Singh, S. K. Singh, V. Gueskine, X. Crispin and M. Berggren, *ACS Appl. Polym. Mater.*, 2019, **1**, 83–94.
14 J. Edberg, D. Iandolo, R. Brooke, X. Liu, C. Musumeci, J. W. Andreasen, D. T. Simon, D. Evans, I. Engquist and M. Berggren, *Adv. Funct. Mater.*, 2016, **26**, 6950–6960.
15 B. S. Tomar, A. Shahin and M. S. Tirumkudulu, *Soft Matter*, 2020, **16**, 3476–3484.

